Simulation of Hamiltonian Function for Contaminant Fluid Flow

I.M. Echi[*1], A. N. Amah,[2] and E. Anthony[3]

[1, 2, 3] Department of Physics, University of Agriculture, Makurdi, Nigeria

ABSTRACT

Hamiltonian function for the transport of contaminants was constructed and simulated for different forms of flow velocities and diffusion models. The flow velocities vary in space and time while the diffusion models are functions of contaminant concentration leading to nonlinearity in the transport equation for the contaminant distribution. Explicit space centre and forward time finite difference approximation was applied to solve the equations. Graphical outputs of the contaminant distribution in space and time for the space varying carrier velocity show that diffusion plays significant role in the contaminant distribution in the half integer and one quarter power models, where the peclet number is greater than unity contrary to the prediction of linear theory. Advection dominates the contaminant distribution only when the peclet number, P_e is of several orders of magnitude greater than unity (P_e =149, [1]229). In the harmonic diffusion models and space varying advection both diffusion and advection contribute to contaminant distribution when $P_e < 1$, which according to linear theory should be diffusion, dominated.

(Keywords: Hamiltonian, Advection, Diffusion, Contaminant and models)

INTRODUCTION

A Hamiltonian form H for a dynamical system is very important in that a number of inquires, and sometimes conclusions can be made about the system without a prior solution of the dynamical equation. For instance, a Hamiltonian functional which is not explicit in time t may lead to autonomous flow with H as one of the integrals of motion. If some coordinates are cyclic in H, the conjugate momenta are also constants of motion.

If H is one dimensional (1-D) and independent of t, then chaotic motions are ruled out [1,2]. The dynamical equations of motion of the state variables ξ_k are furnished by the Hamilton's equations

$$\dot{\xi}_k = \eta \frac{\partial H}{\partial \xi_k} \qquad (1)$$

Where η is an appropriate sympletic structure and $\dot{\xi}_k$ represents derivative of the state variable ξ_k with respect to time [2,3].

There are however, some Hamiltonian functional forms such as ours which though lead to the dynamical equation correctly given by (1) may lack any general conclusion. The difficulties may be due to several reasons. In a purely mathematical abstrictions, all variables in H other the time t is state variable. However, in application some variables may be state variables in the moving particle frame but are independent variables of the same status as t in the observation frame. For example in the observation frame the space variable x may not be a function of time. Under this situation equation (1) will lead to a spatio-temporal dynamics (STD).

Transport of matter in fluids is one where STD has found applications over the years. Analytical solution of transport equation is possible under extreme assumptions such as steady state, laminar flow, constant diffusion[4].

In practice these assumptions are rarely valid for non-guided flows which are by far the most dominant in nature. The removal of these assumptions implies

*Corresponding author
Dr. I.M Echi
Department of Physics
University of Agriculture, Makurdi
Email: iduabae@yahoo.com
Tel: 08053908973

inherent non-linearity in the transport equations and an invitation to computer simulations.

A lot of advances have been made in recent years in the simulation of non-linear spatio-temporal transport equations and their applications in environmental pollution[5-8]. Nonlinearity may enter the transport equations through the carrier flow velocity, the diffusive term, and the source and sink models among others.

The Peclet number is another important non-dimensional term which compares the characteristic time for dispersion and diffusion given a length scale with the characteristic time for advection [9]. This is given by

$$P_e = \frac{uL}{D} \qquad (2)$$

where u is the velocity of fluid flow, L is the characteristic length scale and D is the diffusion coeffiecient [10].
In practice the values of the diffusion and advection coefficients vary widely from one river to another. The precision of the numerical solution of these models depend on the transport nature: advection dominant ($P_e > 1$) or diffusion dominant ($P_e < 1$) [11,12].

In this paper we constructed a Hamiltonian for the transport equation and simulate the equation for different forms of flow velocities and diffusion factors.

THEORETICAL CONSIDERATION

The Hamiltonian of the transport equation is given by

$$H = -\frac{1}{2}uC^2 + CD\frac{\partial C}{\partial x} - \int D\left(\frac{\partial C}{\partial x}\right)^2 dx - \lambda \int C^2 dx \qquad (3)$$

In application, C may represent the contaminant concentration in a moving fluid of velocity u, x is the spatial coordinate, is the decay strength while D is the diffusion coefficient. The time evolution of C is given by the analogous form of the canonical equation (1):

$$\dot{C} = J\nabla_x H \qquad (4)$$

where the symplectic matrix $J = \frac{1}{C}$ is a 1x1 matrix, and $\nabla_x = \frac{\partial}{\partial x}$. Equation (4) correctly gives the transport equation

$$\frac{\partial C}{\partial t} = -u\frac{\partial C}{\partial x} + \frac{\partial}{\partial x}\left(D(C)\frac{\partial C}{\partial x}\right) - \lambda C \qquad (5)$$

If the flow velocity is uniform. This result can easily be extended to 2-D. If v is the flow velocity in the y-direction then

$$\frac{\partial C}{\partial t} = -u\frac{\partial C}{\partial x} - v\frac{\partial C}{\partial y} + \frac{\partial}{\partial x}\left(D(C)\frac{\partial C}{\partial x}\right) + \frac{\partial}{\partial y}\left(D(C)\frac{\partial C}{\partial y}\right) - \lambda C \qquad (6)$$

Half Integer Diffusion Model

We assumed a diffusion model of the form

$$D(C) = \alpha\sqrt{C} \qquad (7)$$

We let the x-direction be the wind direction so that there is no advection in the y-direction but diffusion is retained in both directions. Here α is a consistent diffusion parameter

Using equation (7) in (6) the transport equation for above model becomes

$$\frac{\partial C}{\partial t} = -u\frac{\partial C}{\partial x} + \alpha\left(\frac{1}{2}C^{-\frac{1}{2}}\left(\frac{\partial C}{\partial x}\right)^2 + C^{\frac{1}{2}}\frac{\partial^2 C}{\partial x^2} + \frac{1}{2}C^{-\frac{1}{2}}\left(\frac{\partial C}{\partial y}\right)^2 + C^{\frac{1}{2}}\frac{\partial^2 C}{\partial y^2}\right) - \lambda C \qquad (8)$$

The One-Quarter Power Model

The One-Quarter Power model is of the form

$$D(C) = \beta C^{\frac{1}{4}} \qquad (9)$$

The transport under similar assumptions as in the half integer model becomes

$$\frac{\partial C}{\partial t} = -u\frac{\partial C}{\partial x} + \beta\left(\frac{1}{4}C^{-\frac{3}{4}}\left(\frac{\partial C}{\partial x}\right)^2 + C^{\frac{1}{4}}\frac{\partial^2 C}{\partial x^2} + \frac{1}{4}C^{-\frac{3}{4}}\left(\frac{\partial C}{\partial y}\right)^2 + C^{\frac{1}{4}}\frac{\partial^2 C}{\partial y^2}\right) - \lambda C \qquad (10)$$

where β is yet another consistent diffusion parameter.

The Harmonic Model

We also considered a unit amplitude oscillating model of the form

$$D(C) = \sin\rho C \qquad (11)$$

Where ρ is an inverse concentration parameter. The transport equation under this model is

$$\frac{\partial C}{\partial t} - u\frac{\partial C}{\partial x} + \rho\cos\rho C\left(\frac{\partial C}{\partial x}\right)^2 + \rho\cos\rho C\left(\frac{\partial C}{\partial y}\right)^2 + \sin\alpha C\frac{\partial^2 C}{\partial x^2} + \sin\alpha C\frac{\partial^2 C}{\partial y^2} - \lambda C \quad (12)$$

Discretization Sheme

Implicit finite difference schemes are generally known for their unconditional stability in solving linear differential equations [13]. Implicit schemes are however difficult to apply to nonlinear problems because the art of discretization may not remove the nonlinearity in the computational space and therefore linear system of equations cannot be written and solved for nonlinear equations. On the other hand the Courant-Fredrick stability condition $\frac{D\Delta t}{\Delta x^2} \leq 0.5$ for explicit schemes may not hold when applying to nonlinear equations. In the mix of these two problems it is natural to follow 'trial will convince you strategy. We applied explicit space centre and forward time finite difference approximation to equation (8), (10) and (12) . Input parameters were adjusted to ensure that numerical over-floating did not occur before the end of simulation run.

We consider two types of advection velocity for our entire model of the transport equation, one varying in space and the other varying in time, which are given as

$$u = u_0 e^{-\beta x} \text{ and } u = -A\sin\omega t \quad (13)$$

respectfully.

where u_0 and β are constant, A is the amplitude and ω is the angular speed set at $\omega = 90 rads^{-1}$

The spatial exponential decay model in the contaminant carrier advection velocity is intended to describe the practical situation where the speed of a river dwindles as it approaches its bedding planes, while the time oscillating model describes situations where advection velocity may change due to high or low volume of water in the river, occasioned by rainfalls.

RESULTS AND DISCUSSION

Fig. 1-6 show results for the exponential decay form of the advection velocity for the half integer model. Near the middle of the river (Fig. 1), the line of propagation distribution of the contaminants decreases almost uniformly towards the boundary value. Two reasons may account for this. Diffusion may have shifted contaminants out of propagation and secondly, deposition characterized by the mortality factor λ may have reduced the contaminant concentration. Close to the end of transverse boundary (y=0.9268, Fig. 2), there is spatial oscillations in the contaminant distribution near the source ($0 \leq x \leq 0.3$) before it decreases uniformly downstream. The decrease is however, more rapid than when the transverse coordinate was near the centre of the simulation width. This result is expected because very far from the source, diffusion has not taken enough contaminants there, so the little that reaches the location quickly decays to the background downstream. About half way downstream (x=0.4878), the transverse distribution of the contaminant at time t = 0.9 unit (Fig. 3) appears much like a normal distribution with the origin displaced to about x=0.2 unit of length. This becomes flattened after a long time t=1.9608 units at x=0.9756 unit (Fig. 4). The sharp fall and rise in the concentration near the origin and near the end of the transverse direction respectively may be discarded. The numerical scheme is only trying to conform to the boundary conditions at the expense of physical interpretation.

Near the middle of the simulation plane, (x,y) = (0.4878,0.5610), the distribution (Fig. 6) is an exponential decay. Close to the boundary, (x,y) = (0.9268, 0.9756), the distribution (Fig. 5) is also exponential, but at a much slower rate compared to the middle location. Near the boundary, the 'wall' (river bank) might have limited the diffusion of contaminants so that it is only advection and mortality that degrade the concentration in time. This is not the case near the middle where diffusion has no restriction. It is thus not surprising that the decay is more rapid there than near the boundary. The practical implication of this result is that where people drink water from flowing streams, fetching the water far from the banks may contain less contaminant than near the bank.

The peclet number (eqn 2) is

$$P_e = \frac{0.32 \text{ x } 1}{0.009 \text{ x } \sqrt{15}} = 9.18 \quad (14)$$

which is greater than unity and by linear theory, the contaminant distribution should be dominated by advection making the spread of contaminants in the transverse direction to be nearly zero. In practice when contaminants are washed into a river, turbulence and eddy currents in the fluid flow also help to distribute

contaminants in the transverse directions. Non linear models of the transport equation thus appear to describe situations close to practical observation better than linear models.

Fig. 7-13 show results for the temporal oscillatory advection velocity for the half integer model. The downstream contaminant concentration reduces steadily until half the simulation length when strong oscillations begin to occur (Fig. 7-8). Even though the advection velocity is oscillatory in time, the left boundary, x=0, remains a node. It thus takes several spatial steps for the distribution to de-tune from the nodal condition and follow the oscillating form of the advection velocity. The transverse contaminant distribution sampled at x = 0.5366 and x= 0.9512 for early time, t=0.9020 and late time, t=1.9608 (Fig. 9-10) appear nearly constant in space. Here the peclet number

$$P_e = \frac{0.52}{0.0009x\sqrt{15}} = 149 \qquad (15)$$

is overwhelmingly greater than unity which mean that the effect of non linearity in the diffusion model is subsumed, leaving advection to dominate the distribution of contaminant in aggrement with the linear model of [14] for P_e ranging from 43 - 415. The time variations of concentration at different locations look interesting. The concentration decreases almost linearly (Fig 11) at (x,y) = (0.3658, 0.4878) while at (x,y)= (0.7317,0.7561) (Fig 12) it begins to oscillate with increasing amplitude after an initial linear decrease. Similarly, near end of the simulation plane (x,y) = (0.9268, 0.9756), the concentration oscillates but with decreasing amplitude (Fig 13). The first and last locations are close to the boundaries so that the oscillating advection either decreases linearly the contaminant concentration or with decreasing oscillating amplitude. Away from the boundary and with the neglect of diffusion, the concentration of contaminants at such location may increase or decrease with fluctuating amplitudes in complete respond to the advection fluctuations.

Fig 14-16 show the results for the exponential decay form of the advection velocity for the one quarter model. The peclet number for the exponential decay advection velocity is

$$P_e = \frac{0.26}{0.09 \text{ x } \sqrt[4]{15}} = 1.468 \qquad (16)$$

It is of the same order of magnitude as in the half-integer model. The contaminant distribution follows the same pattern as for the half-integer model with diffusion accounting for the near normalized transverse concentration distribution (compare Fig 1- 3 with Fig 14-16 respectively). The peclet number for the oscillation advection velocity Fig 17-18 is

$$P_e = \frac{0.53x1}{0.0009 \text{ x } \sqrt[4]{15}} = 299 \qquad (17)$$

This is even much greater than when P_e was 149 in the half integer model, with similar oscillating advection velocity. One expects that the diffusion concentration is further suppressed. These are clearly the situations when one compares Fig 18 with Fig 10. In Fig 18 one sees that transverse concentration distribution is almost parallel to the coordinate axis while it was linearly decreases with a gradient of about 1.1 units/m in Fig 10. The oscillations in the contaminant concentration in downstream direction begins at about x=0.2 units with five clear peaks before the boundary (Fig 17) compared with that of Fig 8 which start about x=0.55 and had three clear peaks before the boundary.

Fig. 19-24 show results for the harmonic model.

The peclet number for the exponential decay form of advection velocity,

$$P_e = \frac{0.1}{1} = 0.1 \qquad (18)$$

While for the oscillating model of advection,

$$P_e = \frac{0.4}{1} = 0.4 \qquad (19)$$

In both cases $P_e < 1$. According to linear theory, diffusion should suppress advection. This is not exactly true for our model. However there is faster exponential decay of concentration in the downstream coordinate (Fig 19) and nearly steady concentration maintained across the transverse direction (Fig 20). This corresponds to strong diffusion. At a much longer time t =1.9661 units (Fig 21), the lateral concentration distribution has reduced drastically but still maintains a steady value. This model predicts rapid reduction of contaminant concentration in both directions. The peclet number P_e, even though less than unity, the diffusion was not so dominant as to make the transverse distribution fluctuates in space. Alternatively, the nonlinearity in the diffusion model is not an explicit function of the space coordinates but that of concentration. This may explain why the transverse distribution is not harmonic in space. However for the same harmonic diffusion model and oscillatory advection ($P_e = 0.4$), the concentration oscillates in the downstream direction (Fig 22) while strong diffusion

maintains the concentration at a high steady value in the lateral direction initially (Fig 23) t=0.4878 units and at a much lower steady value after a longer time, t=1.9608 units (Figs 24).

CONCLUSION

The Hamiltonian H given in equation (3) together with the sympletic matrix J yields the contaminant transport equation (5). Due to non linearity in the transport equation , the simulation results for the half and one-quarter diffusion models show that diffusion plays significant role in the contaminant distribution even though the peclet number P_e is greater than unity, which by linear theory should be advection dominated. Similarly, in the harmonic diffusion models it was found that for $P_e < 1$, contaminant transport by advection is not negligible contrary to linear theory results. The simulation results also show that contaminant concentration is higher at the bank of the streams (rivers) than far from the bank, probably due to limitation in the diffusion directions.

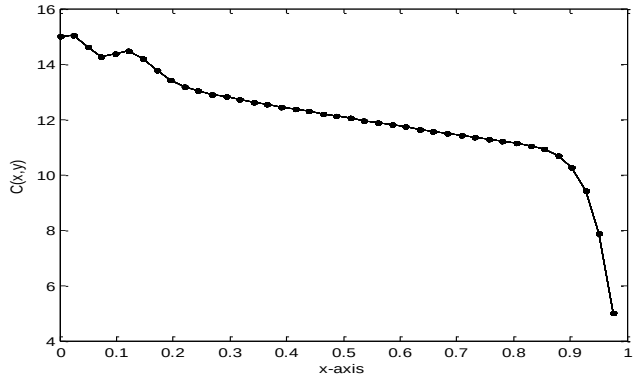

Fig 1: Distribution of contaminants concentration c(x,y) along the downstream direction x, (y,t)=(0.4878,0.9804) parameters u_0=0.32, β=0.2, α=9.0 x10^{-3}, b=0.01

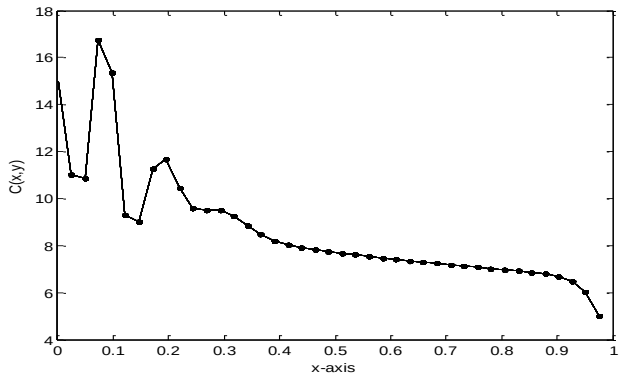

Fig 2: Distribution of contaminants concentration c(x,y) along the downstream direction x (y,t)=(0.9268,1.961), Parameters u_0=0.32, β=0.2, α=9.0 x10^{-3}, b=0.01

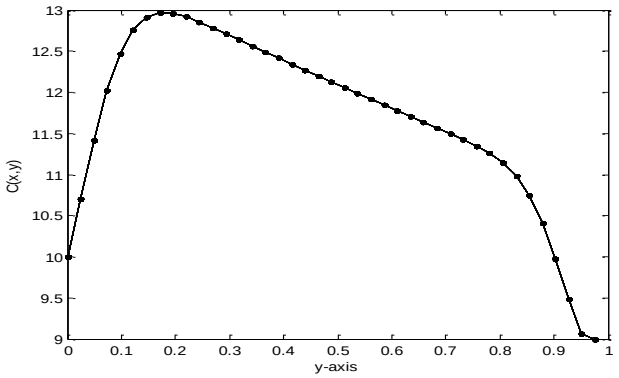

Fig 3: Distribution of contaminants concentration c(x,y) along the transverse direction y (x,t)=(0.4878,0.9804), Parameters u_0=0.32, β=0.2, α=9.0 x10^{-3}, b=0.01

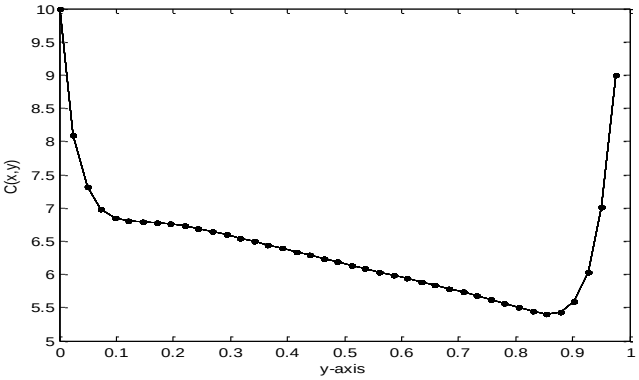

Fig 4: Distribution of contaminants concentration c(x,y) along the transverse direction y (x,t)=(0.9756,1.9608), parameters u_0=0.32, β=0.2, α=9.0 x10^{-3}, b=0.01

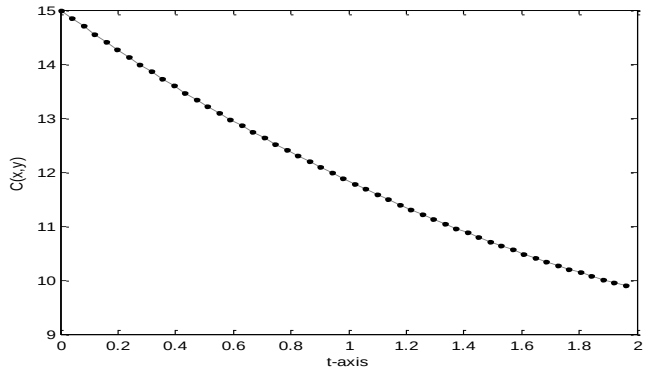

Fig 5: Time variation of contaminants distribution at two fix locations (x,y)=(0.4878,0.5610), parameters u_0=0.32, β=0.2, α=9.0 x10^{-3}, b=0.01

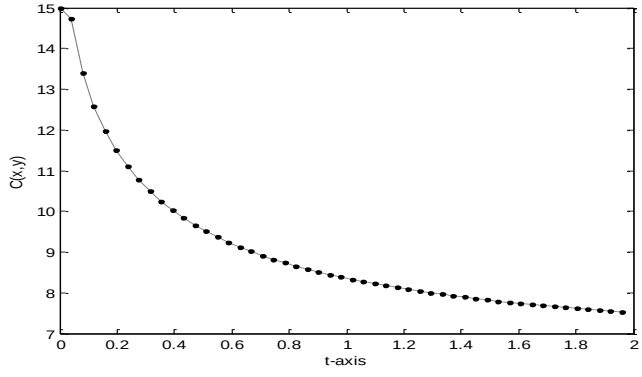

Fig 6:Time variations of contaminants distribution at two fix locations (x,y)=(0.9268,0.9756), parameters u_0=0.32, β=0.2, α=9.0 x10^{-3}, b=0.01

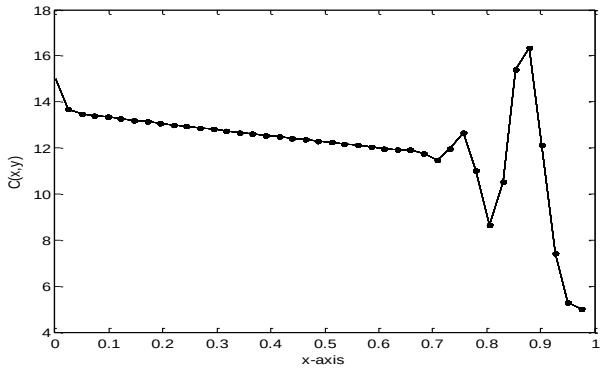

Fig 7: Distribution of contaminants concentration c(x,y) along the downstream direction x (y,t)=(0.4878,0.9412), parameters a=0.52, ω=90rads^{-1}, α=9.0 x 10^{-4}, b=0.009

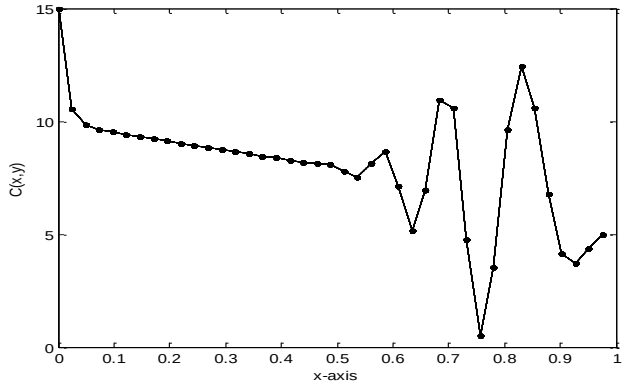

Fig 8: Distribution of contaminants concentration c(x,y) along the downstream direction x (y,t)=(0.9268,1.9608), parameters a=0.52, ω=90rads^{-1}, α=9.0 x 10^{-4}, b=0.009

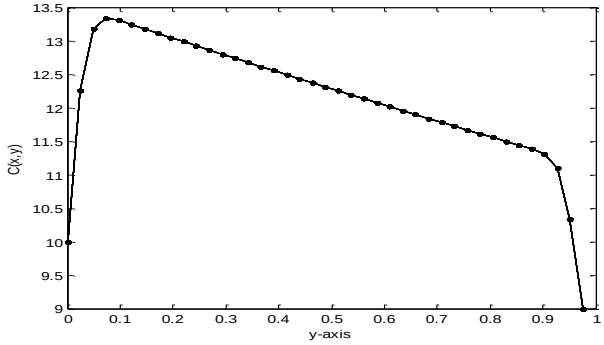

Fig 9: Distribution of contaminants concentration c(x,y) along the transverse direction y (x,t)=(0.5366,0.9020), parameters a=0.52, ω=90rads^{-1}, α=9.0 x 10^{-4}, b=0.009

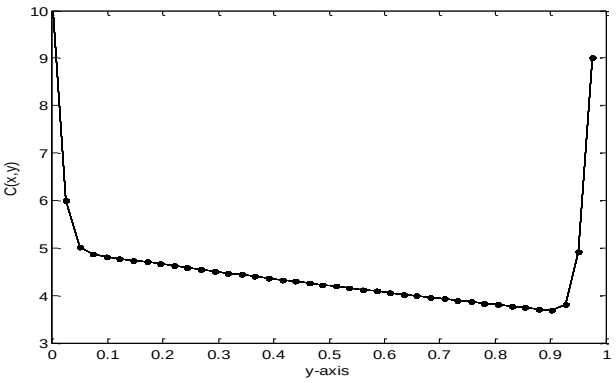

Fig 10: Distribution of contaminants concentration c(x,y) along the transverse direction y (x,t)=(0.9512,1.9608), parameters a=0.52, ω=90rads^{-1}, α=9.0 x 10^{-4}, b=0.009

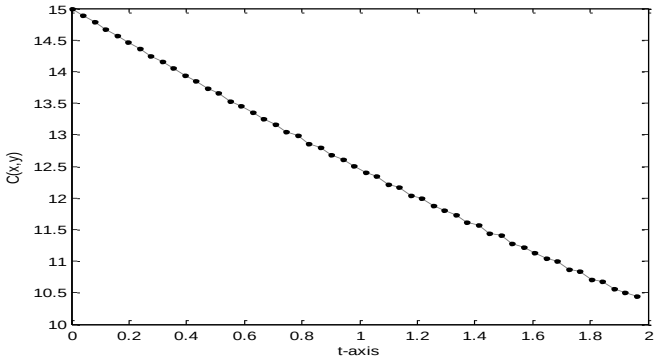

Fig 11: Time variations of contaminants distribution at two fix locations (x,y)=(0.3658,0.4878), parameters a=0.52, ω=90rads^{-1}, α=9.0 x 10^{-4}, b=0.009

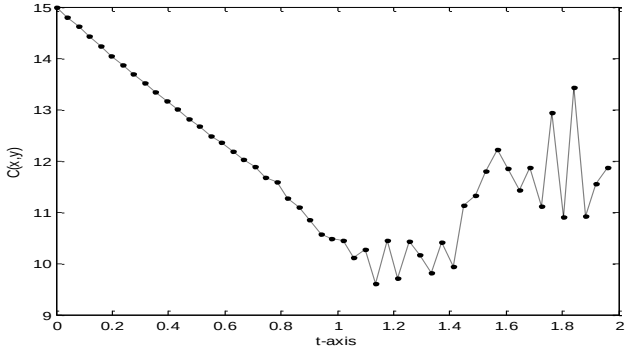

Fig 12: Time variations of contaminants distribution at two fix locations (x,y)=(0.7317,0.7561), parameters a=0.52, ω=90rads^{-1}, α=9.0 x 10^{-4}, b=0.009

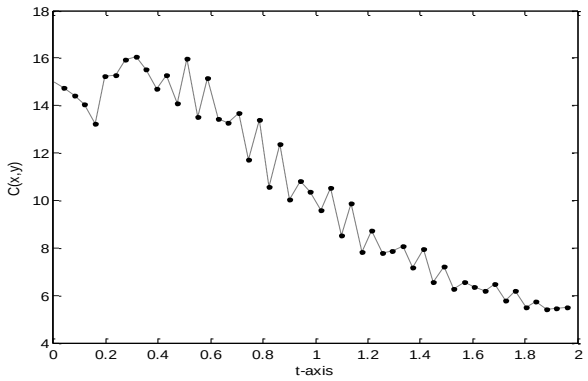

Fig 13: Time variations of contaminants distribution at two fix locations (x,y)=(0.9268,0.9756), parameters a=0.52, ω=90rads^{-1}, α=9.0 x 10^{-4}, b=0.009

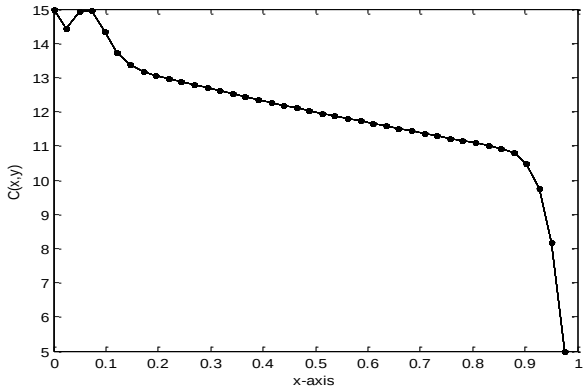

Fig 14: Distribution of contaminants concentration c(x,y) along the downstream direction x (y,t)=(0.4878,0.9804), parameters u_0=0.26, α=0.2, β=9.0 x10^{-2}, b=0.01

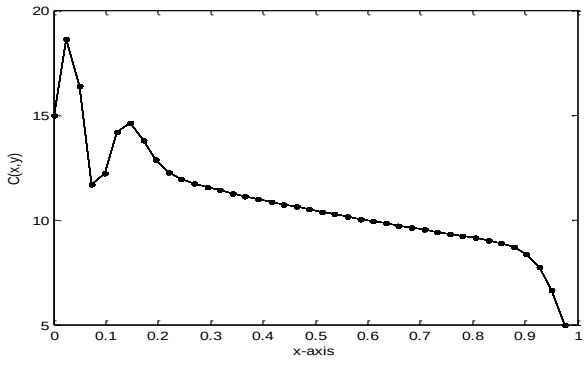

Fig 15: Distribution of contaminants concentration c(x,y) along the downstream direction x (y,t)=(0.5122,1.5686), parameters u_0=0.26, α=0.2, β=9.0 x10^{-2}, b=0.01

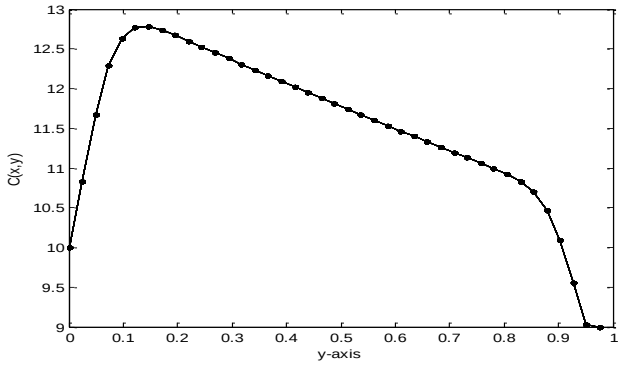

Fig 16: Distribution of contaminants concentration c(x,y) along the transverse direction y (x,t)=(0.5620,0.9804), parameters u_0=0.26, α=0.2, β=9.0 x10^{-2}, b=0.01

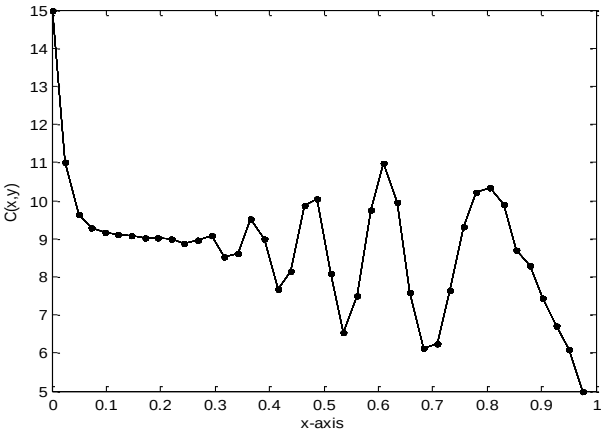

Fig 17: Distribution of contaminants concentration c(x,y) along the downstream direction x (y,t)=(0.9756,2.000), parameters a=0.53, ω=90rads^{-1}, β=9.0 x 10^{-4}, b=0.006

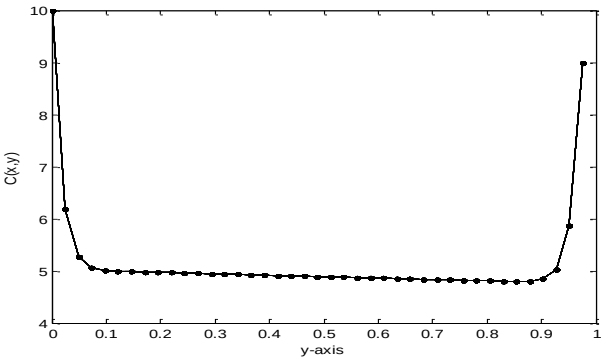

Fig 18: Distribution of contaminants concentration c(x,y) along the transverse y (x,t)=(0.9756, 1.9608), parameters a=0.53, ω=90rads^{-1}, β=9.0 x 10^{-4}, b=0.006

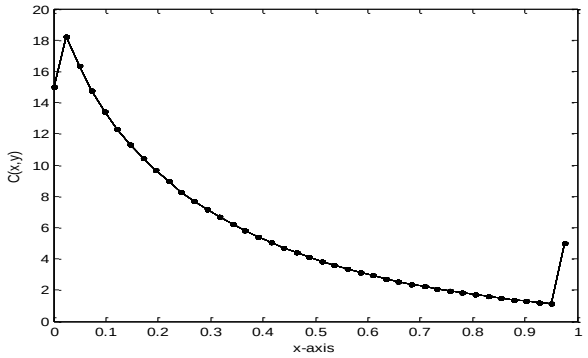

Fig 19: Distribution of contaminants concentration c(x,y) along the downstream direction x (y,t)=(0.9268,1.7647), parameters u_0=0.1, β=0.9, ρ=1.0 x10^{-3}, b=0.01

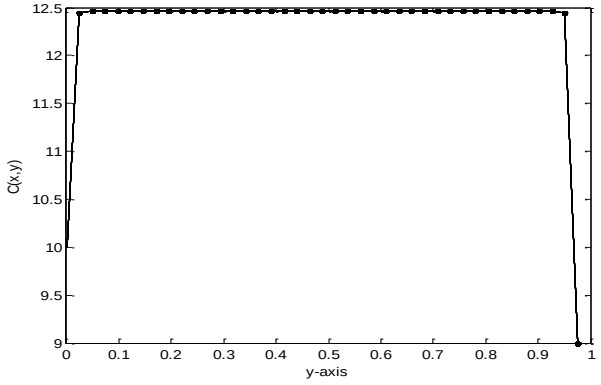

Fig 20: Distribution of contaminants concentration c(x,y) along the transverse direction y (x,t)=(0.3658, 0.3922), parameters u_0=0.1, β=0.9, ρ=1.0 x10^{-3}, b=0.01

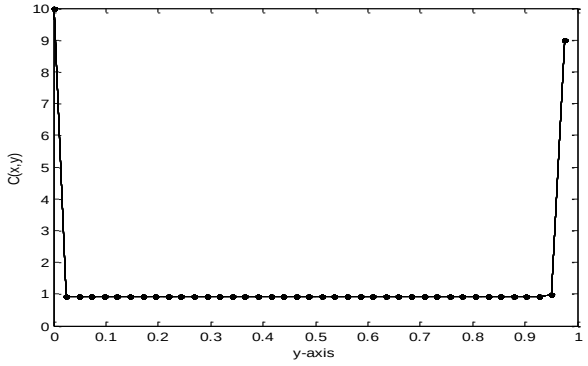

Fig 21: Distribution of contaminants concentration c(x,y) along the transverse direction y (x,t)=(0.9512, 1.9661), parameters u_0=0.1, β=0.9, ρ=1.0 x10^{-3}, b=0.01

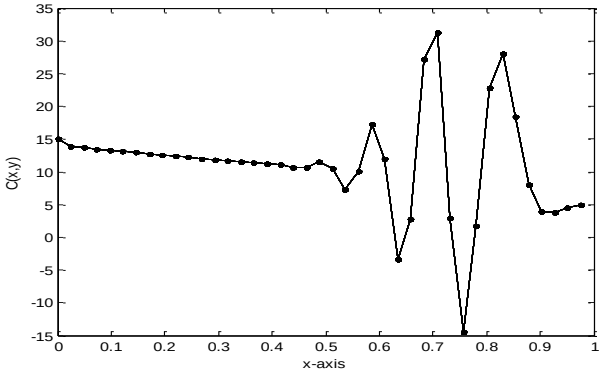

Fig 22: Distribution of contaminants concentration c(x,y) along the downstream direction x (y,t)=(0.9756,1.9608), parameters a=0.4, ω=90rads^{-1}, β=9.0 x 10^{-4}, b=0.006

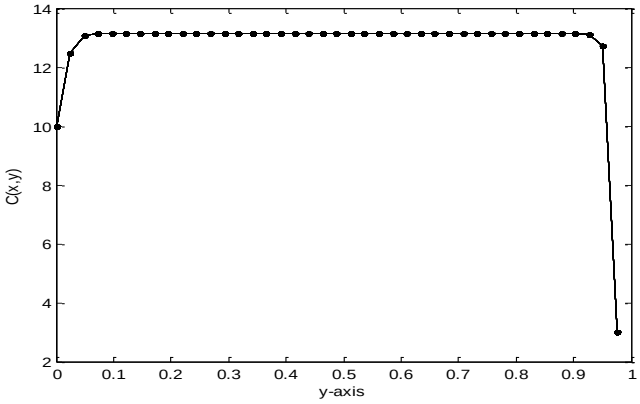

Fig 23: Distribution of contaminants concentration c(x,y) along the transverse direction y (x,t)=(0.4878, 0.9804), parameters a=0.4, ω=90rads^{-1}, β=9.0 x 10^{-4}, b=0.006

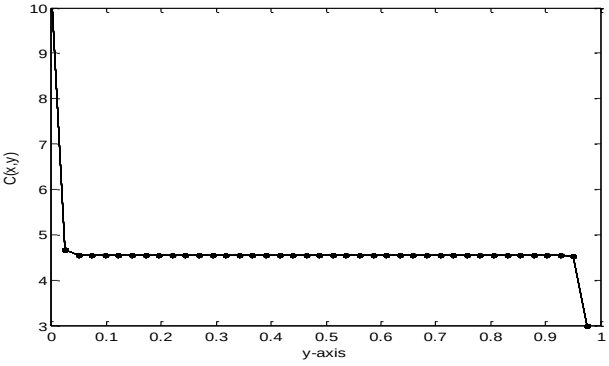

Fig 24: Distribution of contaminants concentration c(x,y) along the transverse direction y (x,t)=(0.9756, 1.9608), parameters a=0.4, ω=90rads^{-1}, β=9.0 x 10^{-4}, b=0.006

References

1. Palacian J. and Yanguas, (2003). From Hamiltonian PDEs to Hamiltonian ODEs Through Normal Forms. Monografias del Semin Matem. Garcia de Galdeano 27, 453-460

2. Robert C. Hilborn, (2004). Chaos and Nonlinear Dynamics. Oxford University Press, United States

3. Walter Craig, (2008). Transformation theory of HamiltonianPDE and problem of water waves. NATO Science for Peace and Security Series B: Springer- Verlag, 67-83

4. Joachim W. Dippner,(2005). Mathematical Modelling of Transport of Pollution in Water. Enclyclopedia of Life Support System (EOSLSS), EOSLSS Publisher, Oxford, Uk.

5. Pawel M. Rowinski, (2008). Constituent Transport in Fresh Surface Water. Enclyclopedia of Life Support System (EOSLSS), EOSLSS Publisher, Oxford, Uk

6. Elisabeta Christina Ani (2010). Modelling of Pollutant Transport in Rivers. Rev. Roum. Chem. 55(4), 284-291

7. Combell L. J and Yiu B, (2006). On Stability of Alternating – Direct Explicity Methods forAdvection Diffusion equations.Wiley Interscience (www.interscience.wiley.com)

8. Watt S. D and Webber R. O (1996). A Reaction Diffusion Equation with a non Constant Diffusivity. J. Austral. Math.Soc. Ser. B37,458-473

9. Murat Sari, Gürhan Gürarslan and Asuman Zeytinoğlu, (2010). High-Order FiniteDifference Schemes for Solving the Advection-Diffusion Equation. Mathematical and Computational Applications, 15(3), 449-460,

10. Steefel C. I and MacQuarrie K. T. B, (1996). Approaches to modeling reactive transport in porous media. Reviews in Mineralogy 34, 83-125,

11. Cyril Fleurant and Jan van der Lee, (2001). A Stochastic Model of Transport in Three-Dimensional Porous Medi. Mathematical Geology,33(4), 449-475

12. Fenton J. D, (2011). Stable numerical methods for diffusive flows. WATERCOMP ’89 The First Australian Conference on Technical Computing in theWater Industry, elbourne 30 May-1 June 1989, pp 185-189,Retyped in 2011

13. David Scullen (1992): “ Finite Difference Methods for Advection in Variable- velocity Fields” The University of Adelaide Department of AppliedMathematics

14. Hatfield Kirk, Michael Annable, Jaehyun Cho, Rao P.S.C and Harald Klammler (2004). A direct passive method for measuring water andcontaminant fluxes in porous media Journal of Contaminant Hydrology 75, 155– 181